ELSEVIER

Journal of Molecular Liquids 86 (2000) 151–161

journal of MOLECULAR LIQUIDS

www.elsevier.nl/locate/molliq

Localization in a Highly Correlated Potential Landscape

A. Bunde [a], S. Havlin [b], J. W. Kantelhardt [a], S. Russ [a], and I. Webman [b]

[a] *Institut für Theoretische Physik III, Universität Giessen, D-35392 Giessen, Germany*

[b] *Minerva Center and Department of Physics, Bar-Ilan University, Ramat-Gan 52900, Israel*

Abstract

We discuss the localization behavior of quantum particles in a one-dimensional Anderson model with correlated and uncorrelated random potentials. We are interested in the question if a localization-delocalization transition in these systems can occur and what the conditions are that allow for such a transition between localized and extended states. For the particular case of self-affine potential landscapes we show that a localization-delocalization transition reported recently only occurs, if the variance of the potential fluctuations is kept fixed for all system sizes. If no constraints on the variance are imposed, a new type of "strong" localization occurs in self-affine systems. All states are strongly localized in a way different from the usual Anderson localized states.

1 Introduction

In the past decades, the question of localization in disordered systems has attracted much interest, (for reviews see, e.g. [1,2]). In this work, we discuss, how localization is changed, when the disorder is spatially correlated. We focus on one-dimensional systems and consider single-particle electronic wave functions in the tight-binding approximation. In this approximation, the Schrödinger equation becomes

$$E\psi_n = \epsilon_n \psi_n - \sum_j V_{n,n+j}\psi_{n+j}. \tag{1}$$

Here, E is the energy eigenvalue, $|\psi_n|^2$ is the probability to find an electron at site n, ϵ_n are the site potentials and $V_{n,n+j} = V_{n+j,n}$ the hopping terms. The sum runs over all nearest neighbors j. There are several different models, described by Eq. (1).

0167-7322/00/$ - see front matter
PII S0167-7322(99) 00136-1

(i) In the Anderson model with diagonal disorder, the site potentials ϵ_n are random numbers with zero mean, chosen randomly from an interval of width w, i. e. $\epsilon_n \in [-w/2, w/2]$. Here, w is a positive constant determining the degree of the disorder. The hopping terms $V_{n,n+j}$ are set equal to unity. In the most common form of the Anderson model, the site energies ϵ_n are uncorrelated. This model has been thoroughly investigated both analytically [3–9] and numerically [10–14]. The wave functions are all spatially localized in one and two dimensions for any degree of disorder. Apart from the regions near the band edges, the localization length λ scales as

$$\lambda(w) \sim 1/w^2 \tag{2}$$

for small w [1]. Accordingly, $\lambda(w)$ diverges for $w \to 0$, but for sufficiently large systems the eigenfunctions are always localized, if $w > 0$.

(ii) In the Anderson model with off-diagonal disorder, the site potentials ϵ_n are zero, while the hopping terms are chosen randomly, $V_{n,n+j} \in \{1 - \frac{v}{2}, 1 + \frac{v}{2}\}$. Here, all states are localized in $d = 1$ and 2, except at the band center $E = 0$ in two-dimensional systems, where a singular critical state occurs [15,16].

(iii) Similar to (ii) is the quantum percolation model, where all site potentials ϵ_n are zero and the hopping terms $V_{n,n+j}$ are randomly chosen as 1 with probability p and as 0 with probability $1 - p$ [17–20].

(iv) A problem similar to (i) is the vibrational problem, where the wave-function ψ_n is substituted by the vibrational amplitudes u_n of particles with masses m_n coupled by harmonic springs $k_{n,n+j}$ between them [21]:

$$\omega^2 u_n = \sum_j (k_{n,n+j}/m_n) u_n - \sum_j (k_{n,n+j}/m_n) u_{n+j}. \tag{3}$$

This time-independent vibrational equation is an eigenvalue equation with the eigenvectors $u_{n,\alpha}$ and the eigenvalues $E_\alpha = \omega_\alpha^2$. The time-dependent solution for a particle at site n can be constructed as $z_n(t) = \sum_\alpha u_{n,\alpha} \exp[-i\omega_\alpha t]$ with the sum over all eigenvalues of Eq. (3). Equation (3) is formally identical to (1), if the ϵ_n are replaced by $\sum_j k_{n,n+j}/m_n$. In ordered systems, (1) and (3) become equivalent, while in disordered systems, vibrating particles can have different values of $\epsilon_n = \sum_j k_{n,n+j}/m_n$.

The common feature of (i)-(iv) with uncorrelated disorder is that all states in $d = 1$ and 2 (except possible singular states at $E = 0$) are localized. In $d = 3$, a critical line of localization-delocalization transitions separates localized states from extended states.

2 The Correlated Anderson Model

In the following, we concentrate on the Anderson model with diagonal disorder (case(i)). There is a growing interest in the special conditions, that allow for extended states in these systems. We like to mention the following systems with correlated disordered potentials. Some general discussion can be found in [22].

(i) The random-dimer model is perhaps the simplest example of a short-range correlated system. The site energies have a binary distribution $\epsilon_n \in \{\epsilon_A, \epsilon_B\}$ and ϵ_A is always assigned to two sites in succession, giving e.g. chains with series of site energies

$$\epsilon_A, \epsilon_A, \epsilon_B, \epsilon_A, \epsilon_A, \epsilon_A, \epsilon_A, \epsilon_B, \epsilon_B, \epsilon_A, \epsilon_A, \epsilon_B, \ldots . \tag{4}$$

It has been theoretically predicted that a small subset of the eigenstates are extended [23]. This has been proven by transfer-matrix methods (see Appendix) for the Anderson model with diagonal disorder [24] and for off-diagonal disorder [25,26]. Experimental evidence for these extended states has recently been gained by transmission measurements on random-dimer semiconductor superlattices [27].

(ii) Extended states occur also in certain one dimensional incommensurate or quasiperiodic systems [28,29]. The site energies are described by a periodic function

$$\epsilon_n = V(n\omega), \tag{5}$$

whose period $2\pi/\omega$ is incommensurate with the lattice periodicity, i.e. ω is an irrational number. Most common is the Harper model [30], where $V(n\omega) = \frac{w}{2}\cos(2\pi n\omega)$. In this model a localization-delocalization transition occurs. All states are extended for $w < 4$ and localized for $w > 4$. At $w_c = 4$, the states are critical.

(iii) Recently, de Moura and Lyra [31,32] considered quantum particles in a self-affine potential landscape, where the local potentials ϵ_n are given by the trace of a fractional Brownian particle with Hurst exponent $H > 0$ [33,34]. They reported, that the states near the center of the band become extended for $H > 1/2$. In this paper, we discuss in detail the origin of this intriguing localization-delocalization transition.

3 Self-affine potential landscapes in $d = 1$

In a self-affine potential landscape the potential at site $n+1$ depends on the potential at site n by

$$\epsilon_{n+1} = \epsilon_n + \delta_n, \tag{6}$$

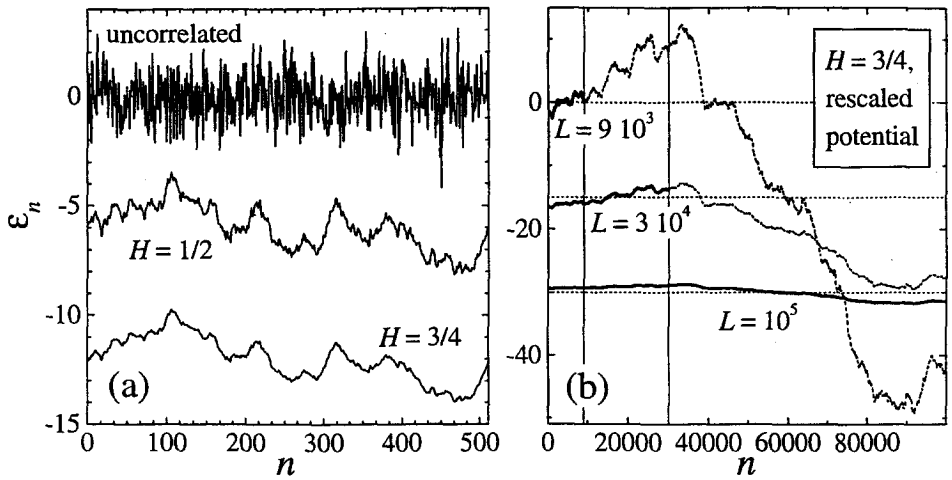

Fig. 1. Illustration of several normalized potential landscapes. In (a) three types of local potentials ϵ_n are shown: Uncorrelated random potential (top line) and self-affine potential landscapes with $H = 1/2$ and $3/4$. The correlated potential landscapes are shifted by integer multiples of 6. The curves in (b) show the same potential landscape with $H = 3/4$, but rescaled such that the variance σ^2 is kept fixed ($\sigma = 1$) for all system sizes considered ($L = 9 \cdot 10^3$, $3 \cdot 10^4$, and 10^5). It is obvious that for increasing system sizes the potential landscape becomes smoother due to the rescaling.

where δ_n is a random number in an interval of width Δ: $-\frac{\Delta}{2} \leq \delta_n \leq \frac{\Delta}{2}$.

(i) If the δ_n are uncorrelated, the ϵ_n are essentially constructed by the trace of a random walk (ϵ_n corresponds to the displacement of a random walker after n steps). Since the mean-square displacement $\langle r^2(t)\rangle$ obeys Ficks law, $\langle r^2(t)\rangle \sim t$, we have

$$\langle(\epsilon_{n+\ell} - \epsilon_n)^2\rangle \sim \ell. \tag{7}$$

(ii) If the δ_n are long-range correlated with a correlation function $\langle\delta_{n+\ell}\delta_n\rangle$ that decays by a power-law, $\langle\delta_{n+\ell}\delta_n\rangle \sim \ell^{-\gamma}$, $0 < \gamma < 1$, the ϵ_n correspond to the trace of a fractional random walk, where $\langle r^2(t)\rangle \sim t^{2H}$ with $H = 1 - \gamma/2$. In this case, we have

$$\langle(\epsilon_{n+\ell} - \epsilon_n)^2\rangle \sim \ell^{2H}. \tag{8}$$

Figure 1 shows, for illustration, potential landscapes for uncorrelated systems (Anderson model) and self-affine systems with $H = \frac{1}{2}$ and $H = \frac{3}{4}$.

In order to decide if a state ψ in this self-affine landscape is localized or extended, one has to determine the localization length λ as a function of the system size L. Practically, one can do this by studying a large system, calculating the localization length and then going

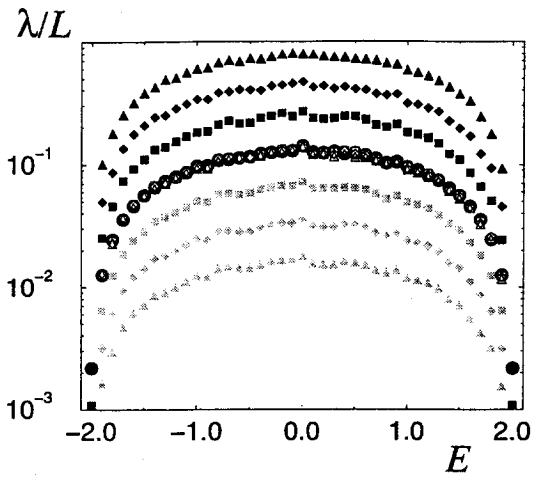

Fig. 2. Analysis of the effect of rescaling of the potentials on an uncorrelated Anderson model in $d = 1$. The relative localization length λ/L is shown as a function of the energy E for chains of different lengths $L = 2^{13}$ (circles), 2^{15} (boxes), 2^{17} (diamonds) and 2^{19} (triangles). We show three sets of chains, corresponding to different rescaling exponents $H = 1/2$ (open symbols), $H = 3/4$ (black symbols), and $H = 1/4$ (grey symbols) for the disorder parameter $w = 0.3(L/2^{13})^{-H}$. The (logarithmic) average of λ was always taken over 1000 systems.

to smaller and smaller sub-systems by cutting the large system into pieces. One usually finds

$$\lambda \sim L^{\alpha}. \tag{9}$$

If $\alpha < 1$, then λ/L decreases with increasing system size and the state is localized, while for $\alpha \geq 1$, the state is extended. Since for self-affine potential landscapes the fluctuations of the potential increase with increasing length scale ℓ according to (8), the variance σ^2 increases with increasing system size L as

$$\sigma^2 \sim L^{2H}. \tag{10}$$

In order to achieve a constant variance of the potential fluctuations, de Moura and Lyra [31,32] rescaled the potential landscapes such that

$$\sigma^2 \equiv \langle \epsilon_n^2 \rangle - \langle \epsilon_n \rangle^2 \equiv \frac{1}{L} \sum_{n=1}^{L} \epsilon_n^2 - \left(\frac{1}{L} \sum_{n=1}^{L} \epsilon_n \right)^2 = 1. \tag{11}$$

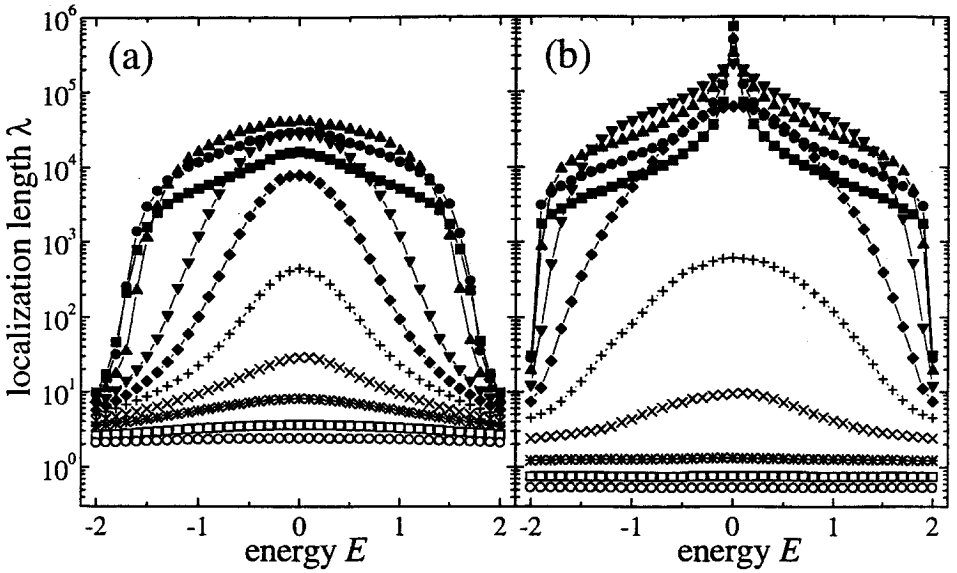

Fig. 3. Plot of the localization lengths λ versus energy E for potential landscapes with (a) $H = 1/2$, $\Delta = 0.04$ and (b) $H = 3/2$, $\Delta = 2 \cdot 10^{-6}$. The symbols indicate the system sizes $L = 2^{11}$ (boxes), 2^{12} (discs), 2^{13} (triangles up), 2^{14} (triangles down), 2^{15} (diamonds), 2^{16} (pluses), 2^{17} (crosses), 2^{18} (stars), 2^{19} (squares), and 2^{20} (circles). The (logarithmic) average of λ was always taken over 1000 configurations.

This normalization condition implies that the rescaled ϵ_n become size-dependent with

$$\epsilon_n \to \frac{\epsilon_n}{L^H} \tag{12}$$

for a system of size L. The effect of rescaling can be best seen in the Anderson model with diagonal disorder, where $w = w_0/L^H$. Without rescaling it is well-known that all states are localized. But, using Eq. (12), we obtain for the localization length of the rescaled system:

$$\lambda \sim 1/w^2 \sim (1/w_0^2) L^{2H}. \tag{13}$$

This equation implies (according to (9)) that extended states occur for $2H > 1$, i.e. $H > \frac{1}{2}$. Numerical calculations by transfer-matrix techniques yield the same result as Eq. (13) and give extended states for $H > \frac{1}{2}$. This is shown in Fig. 2, where the relative localization length λ/L is plotted as a function of the energy E for chains of different lengths L and three values of H. The set of data with $H = 1/2$ can be interpreted as the "critical" case, because λ/L is independent of the system size L. For $H > 1/2$, λ increases faster than L, while for $H < 1/2$, λ increases slower than L.

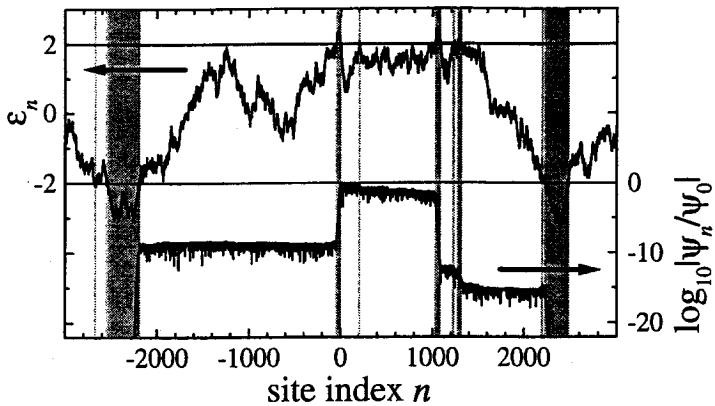

Fig. 4. Example of a strongly localized wave function with $E \approx 0$ in a potential landscape with $H = 1/2$ and $w = 0.1$, where several on-site potentials ϵ_n (shaded) are larger than $E + 2$ or smaller than $E - 2$. It can be seen that these potentials cause a sudden drop of the amplitude.

This means that from a pure numerical treatment (we obtained analogous results from level statistics), we were led to postulate the existence of a localization-delocalization transition in $d = 1$ for electrons in random potential landscapes. Of course, the occurence of such a localization-delocalization transition is a pure artefact of the rescaling, which implies that the potentials become locally smoother with increasing system size.

4 Results in self-affine potential landscapes

As we show in the following, the situation is similar for the self-affine potential landscapes. When the normalization condition (11) is imposed, the *local* fluctuations of the potentials decrease with increasing system size as illustrated in Fig. 1(b). This creates apparent "extended" states for $H > 1/2$. Without rescaling, the local fluctuations remain the same and the disorder width w increases with increasing system size L (see Eqs. (10) and (11)) resulting in *strongly* localized states for all correlation exponents H.

Let us first consider non-rescaled self-affine potential landscapes. Figure 3 shows, for $H = 1/2$ ((a), generated by summing up random numbers) and $H = 3/2$ ((b), generated by summing up potentials of (a)), the localization lengths $\lambda(E)$, calculated with the transfer-matrix method for several system sizes L. For small L and E near the band center, $\lambda(E)$ increases with L, but slower than linearly in L. This indicates weakly localized states. For large L and at the band edges, however, this behavior is reversed: $\lambda(E)$ decreases drastically with increasing L, indicating *strongly* localized states.

In order to determine the origin of these strongly localized states, let us consider the eigenfunctions. Figure 4 shows a typical eigenfunction for $E \approx 0$ together with the corresponding potential landscape. It can be seen that the eigenfunction amplitude drops

sharply at sites where the local potential ϵ_n exceeds a value of 2 or -2. The drops increase drastically with increasing size of the region where the potential is outside these bounds (see Fig. 4). If the size of the system increases, the fraction of sites with potentials that exceed the bound $|\epsilon_n| = 2$ increases, and the wave function is even more strongly localized. In an infinite system only strongly localized states can occur. For wave functions with eigenenergy $E \neq 0$ the bounds for strong localization are shifted by E and become $|\epsilon_n - E| > 2$. These considerations are valid for all self-affine potential landscapes with $H > 0$. But the "critical" system size, where for the first time the potential of one site exceeds the bound, depends on H.

The strong localization behavior for self-affine potentials that we observe here has to be distinguished from the usual Anderson localization for uncorrelated potentials. In the case of Anderson localization, the wave functions have an irregular structure and their amplitudes decay roughly exponentially. In contrast, in the case of strong localization, the wave functions have a patchy structure, regions of strong and weak localization alternate, and the wave functions decay in a non-exponential manner.

Finally, let us consider the rescaled potential landscapes where the variance σ^2 (see Eq. (11) is kept constant, independent of system size L. It is obvious from the discussions above, that for sufficiently large values of σ all states are strongly localized. For sufficiently small values of σ (and sufficiently large values of H), on the other hand, the fluctuations on small length scales of the rescaled potentials decrease drastically, and we can expect apparent "extended" states. Figure 5 shows the resulting phase diagram in the E-H plane for several values of the variance σ. The critical lines have been obtained by transfer-matrix calculations, investigating the fluctuations of the localization length as described by Deych et al. in [35]. While all states are localized for $H < 1/2$, they become apparently extended for $H > 1/2$ near the band center. The critical lines are axial symmetric to $E = 0$ and the width of the regime of "extended" states decreases with increasing variance σ.

The critical lines can be estimated in the following way: The self-affine potential landscape can be considered as the trace of a one-dimensional random walk with the step length $\delta_n = \epsilon_n - \epsilon_{n-1}$, see Eq. (6). According to random walk theory, the number of "steps" required for reaching a given "distance" $\hat{\epsilon}$ scales as

$$\ell(E) = A(\hat{\epsilon}/\Delta)^{1/H}, \tag{14}$$

where Δ is the mean step length and A is a non-universal constant [34]. We know that the wave functions become strongly localized, when $|\epsilon_n - E|$ exceeds 2 within the system size L. According to Eq. (14) the number of steps required for reaching this bound scales as $\ell(E) = A[(2 \pm E)/\Delta]^{1/H}$. If $\ell(E)$ is smaller than the system size, the states are strongly localized, otherwise they may be extended or weakly localized. For a given system size L, we have therefore a critical energy E_c, where $\ell(E_c) = L$, that separates a regime of strong localization from a regime of weak localization or extended states. When the potentials are rescaled, the mean step length Δ depends on L and the variance σ, $\Delta = B\sigma/L^H$, where

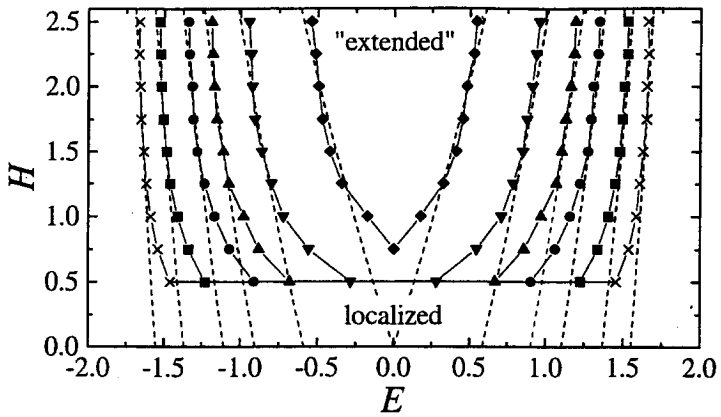

Fig. 5. Phase diagram for the Anderson model with rescaled self-affine potentials generated by Fourier transform (similar to [31]). The transition from apparently extended states to localized states is shown in the H-E plane for six disorder strengths, $\sigma^2 = 0.05$ (crosses), 0.1 (boxes), 0.2 (circles), 0.3 (triangles up) 0.5 (triangles down), 1.0 (diamonds). The theoretical curves, Eq. (15) with $A = 1.15$ and $B = 2$, are included in the figure for each σ. For $H < 1/2$, apparently extended states do not appear.

B is a constant that may depend on the way the correlated potentials are generated numerically. Inserting $\Delta = B\sigma/L^H$ into the relation $\ell(E_c) = A[(2 \pm E_c)/\Delta]^{1/H} = L$, we obtain for the critical energy E_c

$$E_c = \pm(2 - \sigma B/A^H). \tag{15}$$

Figure 5 shows, that this simple relationship describes surprisingly well the dependence of E_c, both on the variance σ and the Hurst exponent H. Below $H = 1/2$, the localization lengths increase slower than the system size L, which is characteristic for weakly localized states. In addition to the localization-delocalization transition for $H \geq 1/2$, further transitions between weakly localized states may occur at small H values.

5 Appendix: Transfer-Matrix Technique

For determining the localization behavior of the eigenstates of Eq. (1), we employed the transfer-matrix method [36,37]. In the transfer-matrix algorithm, one writes Eq. (1) as recursion equation in matrix form:

$$\hat{M}_n \cdot \begin{pmatrix} \psi_n \\ \psi_{n-1} \end{pmatrix} = \begin{pmatrix} \psi_{n+1} \\ \psi_n \end{pmatrix}, \qquad \text{with} \quad \hat{M}_n = \begin{pmatrix} E - \epsilon_n & -1 \\ 1 & 0 \end{pmatrix}, \tag{16}$$

The inverse localization length is defined by

$$\lambda(E)^{-1} = \lim_{N\to\infty} \frac{1}{N} \ln |\frac{\psi_N}{\psi_0}|. \tag{17}$$

It can be shown [37] that in the limit of $N \to \infty$ the ratio ψ_N/ψ_0 is identical to one of both eigenvalues of the product matrix

$$\hat{M}^{(N)} = \prod_{n=1}^{N} \hat{M}_n. \tag{18}$$

Hence, by diagonalizing the matrix $\hat{M}^{(N)}$, we obtain the localization length λ. In our numerical studies, we determined the localization lengths $\lambda^{(\nu)}$ for 1000 configurations, $\nu = 1, ..., 1000$. For obtaining the typical value λ_{typ}, we averaged the $\lambda^{(\nu)}$ logrithmically,

$$\lambda_{\text{typ}} \equiv \exp\left[\frac{1}{N}\sum_{\nu=1}^{N} \ln \lambda^{(\nu)}\right]. \tag{19}$$

We thank the German Israeli Foundation and the Minerva Foundation for financial support.

References

[1] B. Kramer and A. MacKinnon, Rep. Prog. Phys. **56** (1993) 1469.

[2] M. Janssen, Phys. Rep. **295** (1998) 1.

[3] R. E. Borland, Proc. Roy. Soc. London, Ser. A **274** (1963) 529.

[4] B. I. Halperin, Phys. Rev. A **139** (1965) 104.

[5] H. Kunz and B. Souillard, Commun. Math. Phys. **78** (1980) 201.

[6] M. Kappus and F. Wegner, Z. Phys. B **45** (1981) 15.

[7] F. Delyon, H. Kunz, and B. Souillard, J. Phys. A **16** (1983) 25.

[8] B. Derrida and E. Gardner, J. Phys. (Paris) **45** (1984) 1283.

[9] E. J. Gardner, C. Itzykson, and B. Derrida, J. Phys. A **17** (1984) 1093.

[10] A. MacKinnon and B. Kramer, Z. Phys. B **53** (1983) 1.

[11] J. L. Pichard, J. Phys. C **19** (1986) 1519.

[12] M. Schreiber and H. Grussbach, Phys. Rev. Lett. **67** (1991) 607.

[13] E. Hofstetter and M. Schreiber, Phys. Rev. B **49** (1994) 14726.

[14] K. Slevin and T. Ohtsuki, Phys. Rev. Lett. **82** (1999) 382.

[15] C. M. Soukoulis, I. Webman, G. S. Grest, and E. N. Economou, Phys. Rev. B **26** (1982) 1838.

[16] A. Eilmes, R. A. Römer, and M. Schreiber, Eur. Phys. J. B **1** (1998) 29.

[17] S. Kirkpatrick and T. P. Eggarter, Phys. Rev. B **6** (1972) 3598.

[18] C. M. Soukoulis, Q. Li, and G. S. Grest, Phys. Rev. B **45** (1992) 7724.

[19] A. Mookerjee, I. Dasgupta, and T. Saha, Int. J. Mod. Phys. B **9** (1995) 2989.

[20] R. Berkovits and Y. Avishai, Phys. Rev. B **53** (1996) R16125.

[21] Y. Akita and T. Ohtsuki, J. Phys. Soc. Japan. **67** (1998) 2954.

[22] F. M. Izrailev and A. A. Krokhin, Phys. Rev. Lett. **82** (1999) 4062.

[23] D. H. Dunlap, H.-L. Wu, and P. W. Phillips, Phys. Rev. Lett. **65** (1990) 88.

[24] S. N. Evangelou and E. N. Economou, J. Phys. A **26** (1993) 2803.

[25] J. C. Flores and M. Hilke, J. Phys. A **26** (1993) L1255.

[26] F. M. Izrailev, T. Kottos, and G. P. Tsironis, J. Phys. Cond. Mat. **8** (1996) 2823.

[27] V. Bellani, E. Diez, R. Hey, L. Toni, L. Tarricone, C. B. Parravicini, F. Dominguez-Adame and R. Gómez-Alcalá, Phys. Rev. Lett. **82** (1999) 2159.

[28] A. P. Siebesma and L. Pietronero, Europhys. Lett. **4** (1987) 597.

[29] S. Aubry and G. Andre, Ann. Isr. Phys. Soc. **3** (1980) 133.

[30] H. Hiramoto and M. Kohmoto, Int. J. Mod. Phys. B **6** (1992) 281.

[31] F. A. B. F. de Moura and M. L. Lyra, Phys. Rev. Lett. **81** (1998) 3735.

[32] F. A. B. F. de Moura and M. L. Lyra, Physica A **266** (1999) 465.

[33] J. Feder, *Fractals* (Plenum Press, New York 1988).

[34] A. Bunde and S. Havlin (eds.), *Fractals in Science* (Springer, Heidelberg 1994).

[35] L. I. Deych, D. Zaslavsky, and A. A. Lisyansky, Phys. Rev. Lett. **81** (1998) 5390.

[36] G. Paladin and A. Vulpiani, Phys. Rev. B **35** (1987) 2015.

[37] B. Derrida, K. Mecheri, and J. L. Pichard, J. Phys. (Paris) **48** (1987) 733.